# Differentiating between adult intracranial medulloblastoma and ependymoma using MRI

**Juan Deng**
Department of Radiology, Lanzhou University Second Hospital, Lanzhou
**Caiqiang Xue**
Department of Radiology, Lanzhou University Second Hospital, Lanzhou
**Xianwang Liu**
Department of Radiology, Lanzhou University Second Hospital, Lanzhou
**Shenglin Li**
Department of Radiology, Lanzhou University Second Hospital, Lanzhou
**Junlin Zhou** (ery_zhoujl@lzu.edu.cn)
Department of Radiology, Lanzhou University Second Hospital, Lanzhou

**Research Article**

**Keywords:** adult medulloblastoma, ependymoma, magnetic resonance imaging, diffusion-weighted imaging, apparent diffusion coefficient

**Posted Date:** May 31st, 2022

**DOI:** https://doi.org/10.21203/rs.3.rs-1699245/v1

# Abstract

## Purpose

It is difficult to distinguish between adult intracranial medulloblastomas and ependymomas because of their overlapping imaging manifestations. However, considering their different treatments and prognoses, accurate preoperative differential diagnosis is essential. This study aimed to investigate the value of routine magnetic resonance (MR) examination combined with diffusion-weighted imaging (DWI) in the differential diagnosis of adult intracranial medulloblastomas and ependymomas.

## Materials and Methods

MR images of 18 medulloblastomas and 18 ependymomas in adult patients were retrospectively analyzed, and differences in MR features of lesions and apparent diffusion coefficient (ADC) of solid lesions between the two groups were recorded. Independent sample t-tests and $\chi 2$ tests were used to analyze the differences in MR signs and maximum ADC ($ADC_{max}$), minimum ADC ($ADC_{min}$), and mean ADC ($ADC_{mean}$) values between the two groups. The receiver operating characteristic (ROC) curve was used to determine the differential diagnostic efficacy and optimal threshold for each ADC value.

## Results

There were significant differences in age and tumor enhancement between adult medulloblastoma and ependymoma ($P < 0.05$). The $ADC_{max}$ ($0.69 \pm 0.11$ vs. $1.04 \pm 0.20 \times 10^{-3}$ mm²/s, $P < 0.001$), $ADC_{min}$ ($0.57 \pm 0.12$ vs. $0.96 \pm 0.21 \times 10^{-3}$ mm²/s, $P < 0.001$), and $ADC_{mean}$ ($0.62 \pm 011$ vs. $1.00 \pm 0.20 \times 10^{-3}$ mm²/s, $P < 0.001$) values were significantly lower in adult medulloblastoma than in ependymoma. The areas under the ROC curves of $ADC_{max}$, $ADC_{min}$, and $ADC_{mean}$ were 0.951, 0.957, and 0.966, respectively. The optimal $ADC_{mean}$ threshold was $0.75 \times 10^{-3}$ mm²/s, with a sensitivity of 88.9% and a specificity of 88.9%.

## Conclusion

Routine MR imaging examination combined with DWI is helpful in differentiating between intracranial infratentorial medulloblastoma and ependymoma in adults.


## 1 Introduction

Medulloblastoma is one of the most common malignant brain tumors in children, accounting for 8–10% of children's brain tumors (World Health Organization [WHO] grade IV) [1]. In contrast, adult medulloblastoma is extremely rare, accounting for less than 1% of intracranial tumors [2]. Adult medulloblastoma has unique subgroup-specific cytogenetic features that lead to differences in imaging, treatment, and prognosis between them and those in children [3, 4]. Adult medulloblastomas lack characteristic imaging findings and are often misdiagnosed as ependymomas. According to the 2021 WHO classification of tumors of the central nervous system, ependymomas are divided into three grades: WHO grades I–III [5]. There are evident differences in the prognoses of medulloblastomas and ependymomas. Currently, the main treatment for these two conditions is surgical resection. Because medulloblastomas are more malignant than ependymomas and their cerebrospinal fluid disseminates, they require extended radiotherapy after surgery [6]. Therefore, it is important to establish a precise differential diagnosis between the two conditions before surgery.

Magnetic resonance imaging (MRI) is a noninvasive biosafe diagnostic method that plays an important role in the differential diagnosis of brain malignancies and lesions. Conventional MRI techniques, such as T1-weighted imaging (T1W1), T2-weighted imaging (T2WI), fluid-attenuated inversion recovery (FLAIR), and T1 enhancement, are the most common options. Moreover, some studies have reported that diffusion-weighted imaging (DWI) has opened new horizons for the differential diagnosis of certain brain tumors, because more information on the microscopic motion of water protons is provided [7, 8]. The apparent diffusion coefficient (ADC) is a quantitative measure that can be obtained from DWI; it is usually generated by scanner software and is therefore readily available in clinical picture archiving and communication systems. ADC values have previously differentiated pediatric posterior fossa brain tumors, and studies have found significant differences in ADC values between pediatric medulloblastoma and ependymoma [9–11]. However, it has not been used to differentiate adult medulloblastomas from ependymomas.

Therefore, this study aimed to differentially diagnose adult medulloblastoma and ependymoma using conventional MRI and ADC values before surgery to improve the accuracy of preoperative differential diagnosis and guide further clinical treatment.

## 2 Materials And Methods

# 2.1 Patients

This study was approved by the Ethics Committee of the Lanzhou University Second Hospital. The requirement to obtain informed consent was waived, and all data were fully anonymized. The clinical, pathological, and MRI data of adult intracranial medulloblastoma and ependymoma confirmed by surgery and pathology from January 2016 to December 2021 were retrospectively analyzed. The inclusion criteria were as follows: (1) patients aged ≥ 18 years, (2) patients with tumors located in the subtentorial intracranial region, and (3) patients who underwent T1WI, T2WI, FLAIR, and enhanced T1 and DWI before surgery. Finally, 18 (8 men and 10 women; age, 18–67 [average, 30.9] years) patients with adult medulloblastoma were included. Moreover, 18 (11 men and 7 women; age, 18–58 [average, 40.7] years) patients with adult ependymoma were included, including 5 and 13 patients with grade II and III ependymomas, respectively.

# 2.2 Magnetic resonance (MR) imaging

Head MR and enhanced scans were obtained using the German Siemens Verio 3.0 T superconducting MR scanner, with the patients in a supine position. The scanning parameters were as follows: T1WI (gradient echo sequence): repetition time (TR) 550 ms; echo time (TE), 11 ms, layer thickness and spacing, 5.0 mm and 1.5 mm, respectively; field of view (FOV), 260 mm × 260 mm; and matrix, 256× 256; T2WI (turbo spin echo sequence): TR, 2200 ms; TE, 96 ms; layer thickness and spacing, 1.5 mm and 5.0 mm, respectively; FOV, 260 mm × 260 mm; and matrix, 256×256; DWI (spin-echo echo-planar imaging sequence) (frequency selection fat suppression technology): TR, 4000 ms; TE, 100 ms; layer thickness and spacing, 5 mm and 1.5 mm, respectively; FOV, 260 mm × 260 mm; and matrix, 256×256; and T2WI-FLAIR: TR, 9000 ms; TE, 110.0 ms; and layer thickness and spacing, 5 mm and 1.5 mm, respectively. b-values of 0 and 1000 s/mm2 were used in the three orthogonal directions. The contrast agent used was gadolinium-diethylenetriamine-pentaacetic acid. An intravenous bolus injection of 0.1 mmol/kg with a flow rate of 3.0 ml/s was administered, and scanning parameters were all consistent with flat sweep.

## 2.3 Image analysis

Two physicians with more than 10 years of experience in neuroimaging diagnosis performed independent readings in a blinded manner. The location, diameter, shape, cystic change, tumor boundary, peritumoral edema, enhancement uniformity, and degree of enhancement of the tumor were observed and recorded. According to the position occupied by the tumor body, tumors were categorized into “midline” and “non-midline.” The tumor diameter was the maximum diameter of the axial tumor, the morphology was recorded as regular or irregular, and the part of the tumor that was similar to the cerebrospinal fluid signal without enhancement was recorded as cystic degeneration. Moreover, the boundary of the tumor was recorded as clear or blurred according to the observation, peritumoral edema was defined as a hyperintense area on T2WI and FLAIR images that was not enhanced on enhanced scans, and if different degrees of enhancement were observed in 10–90% of the tumor volume, it was inhomogeneous. Regarding tumor enhancement degree, mild enhancement was lower than the cavernous sinus, close to the cavernous sinus, but the intratumoral structure could be identified as moderate enhancement, and the intratumoral structure could not be identified as severe enhancement, recorded as mild-moderate and severe reinforcement. After the DWI scan was completed, the corresponding ADC image was obtained by computer post-processing according to the original DWI image. Regions of interest (ROIs) were drawn on the contrast-enhanced T1-weighted MRI-enhanced area (executive section) and were as centrally located as possible in the tumor; care was taken to avoid cystic, necrotic, and hemorrhagic areas that could affect ADC values. The ROI size was a circle of approximately 30 $mm^2$, and each lesion was measured three to nine times, depending on the size of the lesion [12]. The $ADC_{max}$, $ADC_{min}$, and $ADC_{mean}$ values of each ROI were measured and recorded, and the average value was used for analysis. A consistency analysis was performed on the measurement results of the two physicians.

## 2.4 Statistical analyses

The clinical data and MRI signs of adult intracranial medulloblastomas and ependymomas were statistically analyzed using the Statistical Package for the Social Sciences version 23.0. Interobserver agreement was assessed by calculating the intraclass correlation coefficient (ICC) values for the ADC measurements of the two physicians as follows: ICC < 0.4, poor; 0.59 > ICC ≥ 0.4, fair; 0.75 > ICC ≥ 0.6, good; and ICC ≥ 0.75, excellent [4]. When comparing between groups, the chi-squared test or Fisher's exact test was used for enumeration data, the Kolmogorov–Smirnov test was used to test whether the measurement data conformed to a normal distribution, and the independent samples t-test was used for normally distributed measurement data. Otherwise, the U test was used. Differences were considered statistically significant at P < 0.05. A receiver operating characteristic (ROC) curve was used to evaluate the differential diagnostic abilities of $ADC_{min}$, $ADC_{mean}$, and $ADC_{max}$.

## 3 Results

# 3.1 Clinical and MR features

The age at onset of adult intracranial medulloblastoma was lower than that of adult ependymoma, and the difference between the two groups was statistically significant (P = 0.002). The enhancement degrees of adult medulloblastoma were approximately 72.22% and 27.78% with mild to moderate enhancement and marked enhancement, respectively, whereas those of adult ependymoma were approximately 38.89% and 61.11%, respectively, and the difference was statistically significant (P = 0.044). There were no significant differences in sex, tumor location, shape, maximum tumor diameter, cystic degeneration, tumor boundary, peritumoral edema, or enhancement uniformity between the two groups (P > 0.05) (Table 1, Fig. 1, and Fig. 2).

Table 1
The clinical and conventional magnetic resonance imaging characteristics of adult medulloblastoma and ependymoma

| Clinicoradiological features | Medulloblastoma (n = 19) | Ependymoma (n = 19) | P |
|---|---|---|---|
| Age (years, mean ± SD) | 30.9 ± 12.3 | 40.7 ± 11.6 | 0.002* |
| Sex (male/female) | 8 (10) | 11 (7) | 0.317 |
| Location centerline | 6 (33.33%) | 4 (22.22%) | 0.457 |
| Regular in shape | 4 (22.22%) | 2 (12.50%) | 0.371 |
| Maximal transverse diameter (cm) | 37.60 ± 11.47 | 36.48 ± 15.03 | 0.788 |
| Cysts/necrosis changes – yes | 13 (38.46%) | 17 (94.44%) | 0.074 |
| Peritumoral edema – yes | 4 (22.22%) | 2 (12.50%) | 0.371 |
| Enhancement of uniformity – yes | 3 (16.67%) | 4 (22.22%) | 0.674 |
| Severe enhancement – yes | 5 (27.78%) | 11 (61.11%) | 0.044* |
| Data reported as the number of patients (%) and mean ± SD | | | |
| * = significant | | | |

# 3.2 Apparent diffusion coefficient value

The ICC of the ADC values measured by the two observers was 0.969, indicating excellent agreement. The $ADC_{max}$, $ADC_{min}$, and $ADC_{mean}$ values of adult ependymomas were significantly higher than those of adult medulloblastomas ($P < 0.001$) (Table 2). The areas under the ROC curves of $ADC_{max}$, $ADC_{min}$, and $ADC_{mean}$ were 0.951, 0.957, and 0.966, respectively. When the $ADC_{max}$ threshold was $0.86\times10^{-3}$ mm²/s, the sensitivity and specificity of diagnosing medulloblastoma and ependymoma were 83.3% and 100.0%, respectively. When the $ADC_{mean}$ threshold was $0.57\times10^{-3}$ mm²/s, the sensitivity and specificity of diagnosing medulloblastomas and ependymomas were 88.9% and 88.9%, respectively. When the $ADC_{min}$ threshold was $0.69\times10^{-3}$ mm²/s, the differential diagnosis of adult medulloblastomas and ependymomas was more effective, with sensitivity and specificity of 88.9% and 88.9%, respectively (Table 3, Fig. 3).

Table 2
Comparison of apparent diffusion coefficient $(ADC)_{max}$, $ADC_{mean}$, and $ADC_{min}$ values between adult medulloblastomas and ependymomas

| Group | $ADC_{max}$ ($\times 10^{-3} mm^2/s$) | $ADC_{min}$ ($\times 10^{-3} mm^2/s$) | $ADC_{mean}$ ($\times 10^{-3} mm^2/s$) |
|---|---|---|---|
| Medulloblastoma | 0.69 ± 0.11 | 0.57 ± 0.12 | 0.62 ± 0.11 |
| Ependymoma | 1.04 ± 0.20 | 0.96 ± 0.21 | 1.00 ± 0.20 |
| *t* | −7.014 | −6.863 | −7.283 |
| P | < 0.001* | < 0.001* | < 0.001* |
| * = significant | | | |

Table 3
Diagnostic performance of adult medulloblastomas and ependymomas by different parameters

| Parameter | AUC | Cutoff ($\times 10^{-3} mm^2/s$) | Sensitivity | Specificity |
|---|---|---|---|---|
| **$ADC_{max}$** | 0.951 | 0.56 | 83.3% | 100.0% |
| **$ADC_{min}$** | 0.957 | 0.69 | 88.9% | 88.9% |
| **$ADC_{mean}$** | 0.966 | 0.75 | 88.9% | 88.9% |

# 4 Discussion

MRI is the primary method for the preoperative evaluation of medulloblastomas and ependymomas in adults. Our study found statistically significant differences in age and tumor enhancement between the two patients. In addition, we found that the $ADC_{max}$, $ADC_{mean}$, and $ADC_{min}$ values of medulloblastoma were significantly lower than those of ependymoma. Among them, $ADC_{mean}$ had the highest AUC value of 0.898, and when the cutoff value was $0.75 \times 10^{-3}$ mm²/s, its sensitivity and specificity were 88.90% and 88.90%, respectively. Therefore, conventional MR and ADC values are considered valuable in differentiating medulloblastomas and ependymomas.

## 4.1 Clinical and MR features

First, the present study found that the age of onset of adult medulloblastomas was lower than that of ependymomas. Adult medulloblastomas and ependymomas are relatively rare tumors of the central nervous system. Wong’s study found that the median age at diagnosis of adult medulloblastoma was 27 (range, 19–63) years [4]. Our study showed that the mean age of patients at diagnosis was 30.9 years. Zhao et al. [13] reported that the average age at diagnosis of intracranial ependymoma in adults was

36.2 years. The result of our study is similar to those of previous studies. In addition, we distinguished conventional MR findings of adult medulloblastomas from those of ependymomas. We found a statistically significant difference in the degree of enhancement between the two groups. Adult medulloblastomas were mainly mild-to-moderately enhanced, whereas ependymomas were significantly enhanced. The degree of tumor enhancement is generally related to blood supply to the tumor. There are various enhancement methods and degrees of adult medulloblastoma, which can manifest as no evident enhancement, “cloud flocculent” uneven weak enhancement, evident enhancement of the whole tumor, or rosette enhancement due to evident necrosis and cystic transformation of the tumor. The enhancement methods of medulloblastomas are not only related to the blood supply of the tumor but also to its histological type [14]. Ependymomas, especially anaplastic ependymomas, are tumors with relatively rich blood supplies [15]. Thus, there is less enhancement in adult medulloblastomas than in ependymomas.

# 4.2 Apparent diffusion coefficient value

DWI is a functional MRI technique that can detect the extent of water diffusion in biological tissues [16]. The ADC value can be obtained from DWI and is a quantitative indicator that is negatively correlated with the DWI signal; that is, as the ADC value increases, the diffusion of water molecules accelerates, and the DWI signal decreases [17]. Recently, DWI has made progress in the differential diagnosis of medulloblastomas and ependymomas in the posterior fossa of children. Pierce et al. [18] found that the $ADC_{min}$ value of childhood medulloblastomas was lower than that of other posterior fossa tumors, including ependymomas. When the $ADC_{min}$ threshold value was $0.66×10^{-3}$ mm²/s, the positive and negative predictive values of other tumors were differentiated, and the accuracies were 86%, 97%, and 93%, respectively. Another study showed that the $ADC_{max}$, $ADC_{mean}$, and $ADC_{min}$ values of children’s ependymomas were higher than those of children’s medulloblastomas, and the difference between the $ADC_{max}$ and $ADC_{mean}$ values was significant [19]. Similar results were found by Dury [11], with a cut-off value of $0.96×10^{-3}$ mm²/s for distinguishing between medulloblastomas and ependymomas in children. The results of the present study are similar to those of previous studies, among which $ADC_{mean}$ has the highest discriminative performance, with an AUC value of 0.898 and a cutoff value of $0.71×10^{-3}$ mm²/s, with sensitivity and specificity of 92.9% and 71.4%, respectively. Our study found that the ADC value of adult medulloblastomas was significantly lower than that of adult ependymomas. This may be because adult medulloblastomas are WHO grade IV malignant tumors. Pathology shows many densely packed small round or oval cells with high nuclear-to-cytoplasmic ratios. Molecular diffusion is limited, and dense tumor cells limit the diffusion of water [20]; therefore, the tumor’s ADC value is low. In contrast, ependymomas originate from ependymal cells. Pathologically, the size and shape of tumor cells are similar. The main difference between ependymomas and medulloblastoma is the rich cytoplasm. As the cytoplasm of tumor cells is rich, the nucleocytoplasmic ratio is low, and the cells are relatively small. Medulloblastomas are loose; thus, the limited diffusion of water molecules inside and outside the cell is lighter than that in medulloblastomas. Moreover, DWI has mostly iso- or low signal, and the corresponding ADC value is higher. As a result, the ADC value of adult medulloblastomas is lower than that of ependymomas.

## 4.3 Limitations

This study has certain limitations. First, the sample size was small, and no further grading and typing of the adult medulloblastomas and ependymomas were performed. Because adult medulloblastomas and ependymomas are relatively rare tumors, sample size needs to be expanded in later studies. Second, this was a retrospective study, and there was a certain selection bias. Finally, our study is a preliminary exploration of the identification of adult medulloblastoma and ependymoma, and more advanced techniques will be used to identify the two in later stages.

## 4.4 Conclusion

In conclusion, compared with ependymoma, adult medulloblastoma has a lower degree of MR enhancement, and the ADC value of medulloblastoma tumor parenchyma is significantly lower than that of ependymoma, for which $ADC_{mean}$ is the best indicator. Routine MR signs combined with ADC values have value in differentiating adult medulloblastomas and ependymomas.

# Declarations


### Acknowledgments and Funding

We are grateful to the patients included in this study. We would like to thank Editage (www.editage.cn) for English language editing. This study was funded by Grant No. 82071872 from the National Natural Science Foundation of China.


### Author Contributions

Juan Deng, Caiqiang Xue, and Junlin Zhou conceived and designed the study. Material preparation, data collection, and analysis were performed by Xianwang Liu and Shenglin Li. Juan Deng and Caiqiang Xue drafted the manuscript. All authors contributed to the study conception and design. Juan Deng and Caiqiang Xue contributed equally to this work.

**Availability of data and material:** Available upon reasonable request.

**Ethics approval and consent to participate:** The study was approved by the institutional review board; formal consent is not required for a retrospective and noninterventional study.

**Consent for publication:** The authors affirm that human research participants provided informed consent for the publication of the images in Figs. 1 and 2.

**Conflicts of interest:** The authors declare no competing interests.

# References

1. Merchant TE, Pollack IF, Loeffler JS (2010) Brain tumors across the age spectrum: biology, therapy, and late effects. Semin Radiat Oncol 20 (1):58–66. doi:10.1016/j.semradonc.2009.09.005
2. Majd N, Penas-Prado M (2019) Updates on Management of Adult Medulloblastoma. Curr Treat Options Oncol 20 (8):64. doi:10.1007/s11864-019-0663-0
3. Ruda R, Reifenberger G, Frappaz D, Pfister SM, Laprie A, Santarius T, Roth P, Tonn JC, Soffietti R, Weller M, Moyal EC (2018) EANO guidelines for the diagnosis and treatment of ependymal tumors. Neuro Oncol 20 (4):445–456. doi:10.1093/neuonc/nox166
4. Wong GC, Li KK, Wang WW, Liu AP, Huang QJ, Chan AK, Poon MF, Chung NY, Wong QH, Chen H, Chan DTM, Liu XZ, Mao Y, Zhang ZY, Shi ZF, Ng HK (2020) Clinical and mutational profiles of adult medulloblastoma groups. Acta Neuropathol Commun 8 (1):191. doi:10.1186/s40478-020-01066-6
5. Louis DN, Perry A, Wesseling P, Brat DJ, Cree IA, Figarella-Branger D, Hawkins C, Ng HK, Pfister SM, Reifenberger G, Soffietti R, von Deimling A, Ellison DW (2021) The 2021 WHO Classification of Tumors of the Central Nervous System: a summary. Neuro Oncol 23 (8):1231–1251. doi:10.1093/neuonc/noab106
6. Franceschi E, Frappaz D, Ruda R, Hau P, Preusser M, Houillier C, Lombardi G, Asioli S, Dehais C, Bielle F, Di Nunno V, van den Bent M, Brandes AA, Idbaih A, Domain E (2020) Rare Primary Central Nervous System Tumors in Adults: An Overview. Front Oncol 10:996. doi:10.3389/fonc.2020.00996
7. Marupudi NI, Altinok D, Goncalves L, Ham SD, Sood S (2016) Apparent diffusion coefficient mapping in medulloblastoma predicts non-infiltrative surgical planes. Childs Nerv Syst 32 (11):2183–2187. doi:10.1007/s00381-016-3168-1
8. Rodriguez Gutierrez D, Awwad A, Meijer L, Manita M, Jaspan T, Dineen RA, Grundy RG, Auer DP (2014) Metrics and textural features of MRI diffusion to improve classification of pediatric posterior fossa tumors. AJNR Am J Neuroradiol 35 (5):1009–1015. doi:10.3174/ajnr.A3784
9. Rumboldt Z, Camacho DL, Lake D, Welsh CT, Castillo M (2006) Apparent diffusion coefficients for differentiation of cerebellar tumors in children. AJNR Am J Neuroradiol 27 (6):1362–1369
10. Yamasaki F, Kurisu K, Satoh K, Arita K, Sugiyama K, Ohtaki M, Takaba J, Tominaga A, Hanaya R, Yoshioka H, Hama S, Ito Y, Kajiwara Y, Yahara K, Saito T, Thohar MA (2005) Apparent diffusion coefficient of human brain tumors at MR imaging. Radiology 235 (3):985–991. doi:10.1148/radiol.2353031338
11. Dury RJ, Lourdusamy A, Macarthur DC, Peet AC, Auer DP, Grundy RG, Dineen RA (2021) Meta-Analysis of Apparent Diffusion Coefficient in Pediatric Medulloblastoma, Ependymoma, and Pilocytic Astrocytoma. J Magn Reson Imaging. doi:10.1002/jmri.28007
12. Takayasu T, Yamasaki F, Akiyama Y, Ohtaki M, Saito T, Nosaka R, Takano M, Sugiyama K, Kurisu K (2018) Advantages of high b-value diffusion-weighted imaging for preoperative differential diagnosis between embryonal and ependymal tumors at 3T MRI. Eur J Radiol 101:136–143. doi:10.1016/j.ejrad.2018.02.013
13. Zhao F, Wu T, Wang LM, Zhang J, Zhang H, Li SW, Zhang S, Li P, Wang B, Luo L, Liu PN (2021) Survival and Prognostic Factors of Adult Intracranial Ependymoma: A Single-institutional Analysis of

236 Patients. Am J Surg Pathol 45 (7):979–987. doi:10.1097/PAS.0000000000001669

14. Perreault S, Ramaswamy V, Achrol AS, Chao K, Liu TT, Shih D, Remke M, Schubert S, Bouffet E, Fisher PG, Partap S, Vogel H, Taylor MD, Cho YJ, Yeom KW (2014) MRI surrogates for molecular subgroups of medulloblastoma. AJNR Am J Neuroradiol 35 (7):1263–1269. doi:10.3174/ajnr.A3990
15. Delgado-Lopez PD, Corrales-Garcia EM, Alonso-Garcia E, Garcia-Leal R, Gonzalez-Rodrigalvarez R, Araus-Galdos E, Martin-Alonso J (2019) Central nervous system ependymoma: clinical implications of the new molecular classification, treatment guidelines and controversial issues. Clin Transl Oncol 21 (11):1450–1463. doi:10.1007/s12094-019-02082-2
16. Reis J, Stahl R, Zimmermann H, Ruf V, Thon N, Kunz M, Liebig T, Forbrig R (2021) Advanced MRI Findings in Medulloblastomas: Relationship to Genetic Subtypes, Histopathology, and Immunohistochemistry. J Neuroimaging 31 (2):306–316. doi:10.1111/jon.12831
17. Sun PF, Ma L, Ye BQ, Pei YY (2020) Application of diffusion-weighted imaging combined with apparent diffusion coefficient in differential diagnosis between central neurocytoma and ependymoma. Neuroradiology 62 (4):439–445. doi:10.1007/s00234-019-02342-6
18. Pierce TT, Provenzale JM (2014) Evaluation of apparent diffusion coefficient thresholds for diagnosis of medulloblastoma using diffusion-weighted imaging. Neuroradiol J 27 (1):63–74. doi:10.15274/NRJ-2014-10007
19. Taheri H, Tavakoli MB (2021) Measurement of Apparent Diffusion Coefficient (ADC) Values of Ependymoma and Medulloblastoma Tumors: a Patient-based Study. J Biomed Phys Eng 11 (1):39–46. doi:10.31661/jbpe.v0i0.889
20. Fruehwald-Pallamar J, Puchner SB, Rossi A, Garre ML, Cama A, Koelblinger C, Osborn AG, Thurnher MM (2011) Magnetic resonance imaging spectrum of medulloblastoma. Neuroradiology 53 (6):387–396. doi:10.1007/s00234-010-0829-8

# Figures

### Figure 1

A 28-year-old woman with medulloblastoma of the fourth ventricle. **a–b** Fourth ventricle growth type round long T1, long T2 mass shadow, with cystic degeneration signal inside; **c** T1 enhancement shows uneven enhancement of the tumor, showing moderate patchy enhancement; **d–f** diffusion-weighted imaging (DWI) shows high signal in the solid part, and apparent diffusion coefficient (ADC) signal decreases. **e** Pathological picture (hematoxylin and eosin [H&E], ×200). The tumor cells grow densely; the cells are short spindled and oval shaped, with sparse cytoplasm; and the chromatin is clump-shaped, forming a true rosette structure.

## Figure 2

A 49-year-old woman with ependymoma of the fourth ventricle. **a–b** Fourth ventricle growth type round long T1, long T2 mass shadow, with cystic degeneration signal inside; **c** T1 enhancement shows evident inhomogeneous enhancement; **d–f** shows that the solid part is slightly low signal on DWI, and ADC shows equal and slightly high signal; **e** pathological map (H&E, ×200) shows that the tumor tissue is composed of spindle cells, the tumor cells are arranged in bundles and weavings, the cytoplasm is eosinophilic, the nucleus is spindle-shaped, and mitotic figures are rare.

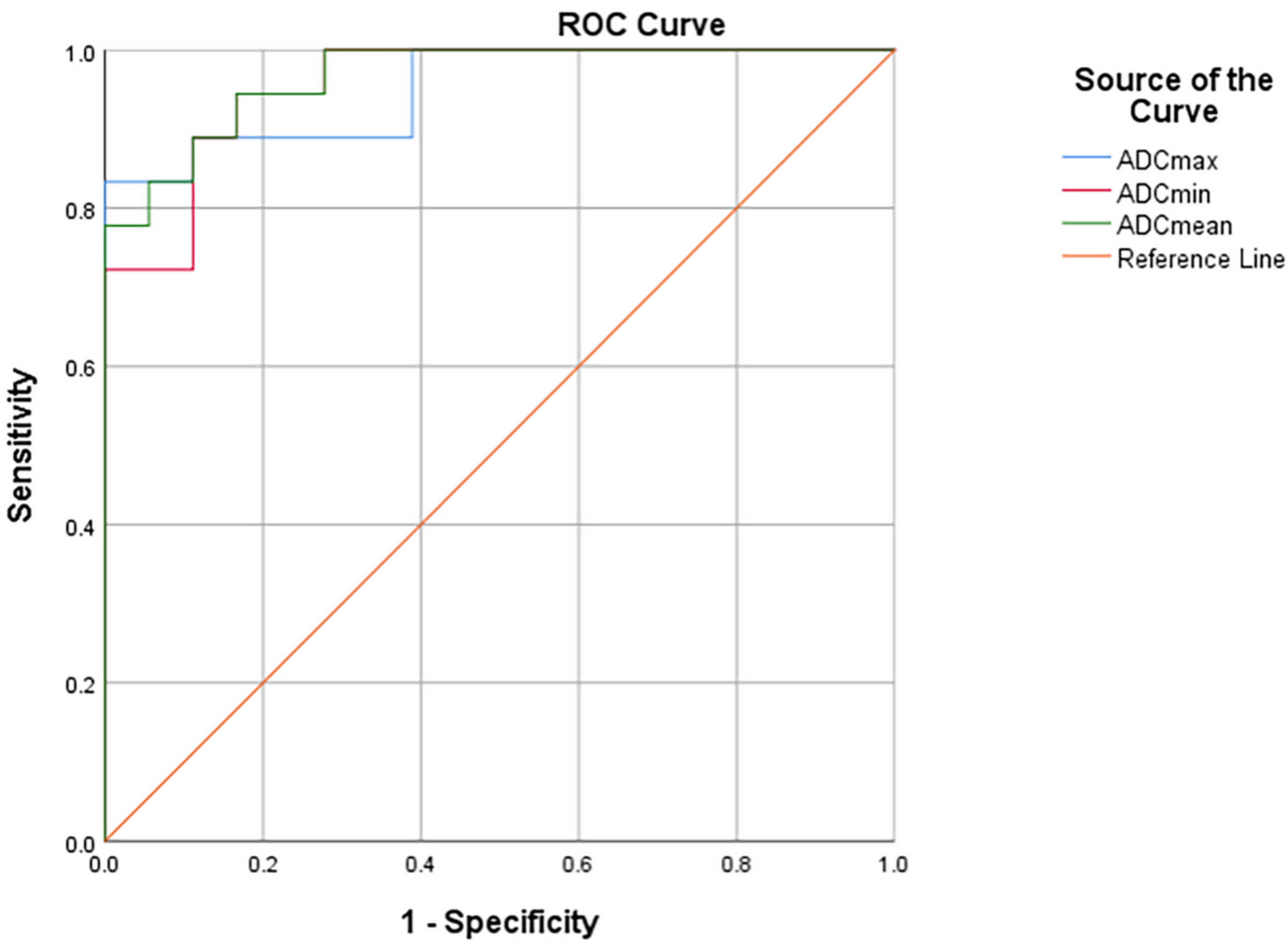


## Figure 3

The $ADC_{max}$, $ADC_{min}$, and $ADC_{mean}$ values differential diagnosis of adult medulloblastoma and ependymoma, and area under the curve is 0.951, 0.957, and 0.966